Applied Water Science (2018) 8:160
https://doi.org/10.1007/s13201-018-0809-4

ORIGINAL ARTICLE

Characterization and application of a 1700-kHz acoustic cavitation field for water decontamination: a case study with toluidine blue

Nor Elhouda Chadi[1] · Slimane Merouani[1,2] · Oualid Hamdaoui[2]

Received: 27 September 2017 / Accepted: 11 September 2018 / Published online: 19 September 2018

Abstract

This work aimed at the characterization and application of a cavitation field induced in water by an ultrasonic reactor operating at 1700 kHz and 15 W. It was found that the size of active bubbles varied from 0.23 to 3 µm. The number of active bubbles increased from 6.1142×10^8 s^{-1} L^{-1} at 25 °C to 4.4684×10^9 s^{-1} L^{-1} at 55 °C. The most active bubbles were those achieving temperature of 4000 K and pressure of 1000 atm at the collapse. The characterized cavitation field removed efficiently toluidine blue (TB), an emerging organic contaminant, through reaction with hydroxyl radical. The best TB-removal rate was obtained under argon saturation, but CO_2 completely suppressed the process. TB degradation rate sensitively enhanced with increasing initial substrate concentration and solution pH, whereas the liquid temperature did not affect the degradation rate. Formic acid, as an organic competitor, reduced considerably the degradation of the pollutant.

Keywords Ultrasound · Cavitation field · Bubble population · Cavitational treatment · Toluidine blue (TB) · Degradation

Introduction

High-power ultrasound (frequency ≥ 100 kHz) has become the focus of a new field, known as sonochemistry, which involves the study of the effects of acoustic waves on chemical systems (e.g., synthesis reactions (Serpone and Colarusso 1994), free radical polymerization (Teo et al. 2009), enzymatic reactions (Malani et al. 2014), photocatalytic reactions (Peller et al. 2003; Kaur and Singh 2007; Bekkouche et al. 2017), Fenton and photo-Fenton reactions (Basturk and Karatas 2014; Verma et al. 2015), electrochemical reactions (Pollet 2010; Sáez et al. 2010)). The central event conducting to sonochemistry is the acoustic bubble. Ultrasound, when passing through a liquid medium, causes mechanical vibration of the liquid. If the liquid medium contains dissolved gas, which will be the case under normal conditions, tiny microbubbles can be formed, grown and violently collapsed by the action of the sound wave. This phenomenon is known as acoustic cavitation (Neppiras 1980). The collapse of the acoustic cavitation bubbles is near adiabatic and generates temperatures of thousands of degrees within the bubbles for a short period of time (Ashokkumar 2011). Under this extreme temperature conditions, highly reactive radicals are generated. For example, if water is the medium, $H^{\cdot}$ and $^{\cdot}OH$ radicals are generated by the homolysis of water vapor inside the bubble. These radicals initiate a gas-phase reactions chain, in which several other reactive species (i.e., $HO_2^{\cdot}$ and O,…) may be formed (Yasui et al. 2005). A parallel reaction pathway exists where volatile solutes may evaporate into the bubble and be pyrolyzed by the high core temperatures. The diffusion of these reactive species in the liquid surrounding the bubble has been used to achieve chemical reactions that include the synthesis of nanomaterials, polymers, degradation of organic pollutants, etc. (Hoffmann et al. 1996; Petrier et al. 1998; Teo et al. 2008; Bang and Suslick 2010; Xue 2016; Merouani and Hamdaoui 2017). Under certain conditions, bubble collapse can also result in light emission, sonoluminescence, originating from the core of the bubble during the final stages of collapse.

Sonication offers three reaction zones: the hot gas phase of the bubble (~ 5000 K), the bubble–solution interface (~ 1900 K) and the bulk of the solution (ambient temperature) (Suslick et al. 1986). The degradation of pollutants

✉ Slimane Merouani
s.merouani@yahoo.fr; s.merouani03@gmail.com

[1] Laboratory of Environmental Process Engineering, Faculty of Process Engineering, University Salah Boubnider – Constantine 3, 25000 Constantine, Algeria

[2] Laboratory of Environmental Engineering, Department of Process Engineering, Faculty of Engineering, Badji Mokhtar – Annaba University, 23000 Annaba, Algeria

upon ultrasound depends on their physicochemical properties. A volatile molecule will be incinerated inside the bubble, while a nonvolatile and hydrophilic molecule will be oxidized by the ejected $^{\cdot}OH$ at the bubble interface and in the bulk of the solution (Pétrier and Francony 1997).

As sonochemistry originates from acoustic cavitation, the characterization of the acoustic field is of fundamental interest to control all physical and chemical effects of ultrasound in aqueous solution. The main characteristics of an acoustic field are the bubble number and size, the maximum bubble temperature and pressure and the chemical bubble yield. Some developed experimental procedures for the characterization of acoustic cavitation bubbles have been recently overviewed by Ashokkumar (2011).

Numerical simulation of acoustic cavitation has shown a significant progress in the last decade (Moholkar et al. 2000a, b; Moholkar and Warmoeskerken 2003; Chakma and Moholkar 2013). However, only several limited studies have attempted to provide a physical explanation to the experimental sonochemical results using analysis based on simulations of cavitation bubble dynamics. For example, Vichare et al. (2000) have analyzed the bubble energy under several sonochemical parameters of frequency, intensity and initial bubble radius. Sivasankar et al. (2007) and Park et al. (2018) have simulated the production of free radicals inside a collapsing bubble to give a mechanistic approach for the sono-oxidation of KI and some trihalomethanes, and similar scenario has been adopted by Nazimudheen et al. (2018) for examining the results of the ultrasound-assisted pre-treatment of leachate before anaerobic digestion.

We have recently developed a theoretical procedure based on cavitation model for the characterization of acoustic cavitation fields (Merouani et al. 2014b). This procedure has been used for determining some interesting characteristics of acoustic bubbles (i.e., bubble dynamics, bubbles size, number of bubbles, bubble core temperatures and pressures, etc.) at variable experimental conditions. In this work, an acoustic cavitation field induced in sonochemical reactor operating at 1700 kHz has been characterized, using our early developed procedure (Merouani et al. 2014b), and then applied for the degradation of a typical water contaminant, toluidine blue (TB), which is a phenothiazine dye that is widely used in fields like medicine, textile and biotechnology (Neelakandeswari et al. 2011; Sridharan and Shankar 2012). Though the degradation of organic pollutants by ultrasound has been widely investigated, the combination between the characterization and the application of the acoustic cavitation field was rarely addressed previously. TB has a mutagenic effect and has a toxic interaction with DNA and RNA (Chi et al. 2010), and thus, any presence of this dye in water will damage aquatic life and human health. Additionally, no data are available about the degradation of this dye by acoustic cavitation. The sensitivity of the cavitational treatment to several operational parameters and additives has been clarified.

Materials and methods

All solutions were prepared using deionized water. Toluidine blue (abbreviation: TB; CAS number: 6586-04-5; UPAC name: 7-Amino-N,N,8-trimethyl-3H-phenothiazin-3-iminium chloride-dichlorozinc, molecular formula: $C_{15}H_{16}ClN_3S{\cdot}0.5ZnCl_2$, molecular weight: 373.97 g mol^{-1}) was supplied by Sigma-Aldrich. All other used reagents (Sigma-Aldrich) are of analytic grade and were used as received.

Batch experiments were conducted in cylindrical jacketed glass reactor equipped with a piezoelectric disk (diameter 2 cm) mounted in bottom of the reactor and emitting irradiation at 1700 kHz. Temperature set was fixed by circulating water through a jacket surrounding the cell and controlled by a thermocouple immersed in the cavitating medium. The solution pH was measured with a Jenway 3505 pH-meter. The acoustic power dissipated in the reactor (15 W) was estimated using the calorimetric method (Mason et al. 1992).

Sonication was carried out using an operating volume of 100 mL. Aqueous samples were taken at fixed time intervals and analyzed with an UV–visible spectrophotometer (JASCO V-730) to determine the concentration of TB ($\lambda_{max} = 626$ nm). To ensure reproducibility, the experiments were repeated three times and the data were averaged (error bars have been included in relevant plots). The concentrations of H_2O_2 during sonolysis were measured iodometrically, as described by Merouani et al. (2010a).

Theoretical package

The theoretical procedure given elsewhere (Merouani et al. 2014b) and summarized in Table 1 has been used for characterizing the 1700-kHz cavitation field. The dynamics of each bubble, the extreme temperatures and pressures developed therein, the production of free radicals and the bubble population (size and number) are the main characteristics to be identified herein. All these parameters have been estimated based on single-bubble sonochemistry model developed by our research group (Merouani et al. 2014c, 2015). This model couples the dynamic of a single bubble (described by the Keller–Miksis equation, Eq. 1 of Table 1) oscillating in water under a sinusoidal acoustic pressure with a chemical kinetics occurring within the bubble at the violent collapse, together with the assumption of isothermal expansion and adiabatic collapse and neglecting mass and heat transfer across the bubble wall. Justification of the adopting model assumptions

Table 1 Basic equations of the model (Merouani et al. 2014a, c)

Bubble dynamics

$$\left(1-\frac{\dot{R}}{c}\right)R\ddot{R}+\frac{3}{2}\left(1-\frac{\dot{R}}{3c}\right)\dot{R}^2=\frac{1}{\rho_L}\left(1+\frac{\dot{R}}{c}+\frac{R}{c}\frac{d}{dt}\right)\left[p_B-P(t)\right] \quad (1)$$

$$p_B=p-\frac{2\sigma}{R}-4\mu\frac{\dot{R}}{R} \quad (2)$$

$$P(t)=p_\infty-P_A\sin(2\pi ft) \quad (3)$$

Pressure in the bubble: $$p=\left[P_v+P_{g_0}\left(\frac{R_0}{R\max}\right)^3\right]\left(\frac{R\max}{R}\right)^{3\gamma} \quad (4)$$

Temperature inside the bubble: $$T=T_\infty\left(\frac{R\max}{R}\right)^{3(\gamma-1)} \quad (5)$$

Chemical kinetics

Production rate of the kth species: $$\dot{w}_k=\frac{dn_k}{Vdt}=\sum_{i=1}^{I}(\upsilon''_{ki}-\upsilon'_{ki})r_i \quad (6)$$

where $k=1,\ldots, K$ (number of species), $i=1, \ldots, N$ (number of reactions)

Reaction rates: $$r_i=k_{f_i}\prod_{k=1}^{K}[X_k]^{\upsilon'_{ki}}-k_{r_i}\prod_{k=1}^{K}[X_k]^{\upsilon''_{ki}} \quad (7)$$

Direct and reverse rate constants: $$k_{f_i}=A_{f_i}T^{b_{f_i}}\exp\left(-\frac{E_{a_{f_i}}}{R_gT}\right) \quad (8)$$

$$k_{r_i}=A_{r_i}T^{b_{r_i}}\exp\left(-\frac{E_{a_{r_i}}}{R_gT}\right) \quad (9)$$

Number of bubbles (N)

$$N=\frac{r_{H_2O_2}}{n_{H_2O_2}+0.5(n_{^{\cdot}OH}+n_{HO_2^{\cdot}})} \quad (10)$$

where $r_{H_2O_2}$ is the experiential production rates of H_2O_2 and $n_{H_2O_2}$, $n_{^{\cdot}OH}$ and $n_{HO_2^{\cdot}}$ are the number of moles of H_2O_2, $^{\cdot}OH$ and $HO_2^{\cdot}$ released by each bubble when it collapses (estimated using the single-bubble sonochemistry model)

Variables description dots indicate time derivatives (d/dt), R is the radius of the bubble, c is the speed of sound in the liquid, p_B is the pressure on the liquid side of the bubble, $P(t)$ is the liquid pressures, ρ_L is the density of the liquid, σ is the surface tension, μ is the liquid viscosity, p is the pressure inside the bubble, p_∞ is the ambient static pressure, P_A is the acoustic amplitude [related to the acoustic intensity I_a as $P_A=(2I_a\rho_Lc)^{1/2}$], f is the sound frequency. P_v is the vapor pressure, P_{g_0} is the initial gas pressure inside the bubble, R_0 is the ambient bubble radius, T_∞ is the bulk liquid temperature, R_{max} is the maximum radius of the bubble, γ is the ratio of specific heats capacities (c_p/c_v) of the vapor/gas mixture, R_g is the universal gas constant, A_{f_i} (A_{r_i}) is the pre-exponential factor, b_{f_i} (b_{r_i}) is the temperature exponent and E_{f_i} (E_{r_i}) is the activation energy

was available somewhere else (Merouani et al. 2014a, c, 2015). The used chemical mechanism consists of series of 73 reversible chemical reactions involving O_2, H_2O, $^{\cdot}OH$, $H^{\cdot}$, O, $HO_2^{\cdot}$, O_3, H_2, H_2O_2, N_2, N, NO, NO_2, NO_3, HNO_2, HNO_3, N_2O, HNO, NH, NH_2, NH_3, N_2H_2, N_2H_3, N_2H_4, N_2O_4 and N_2O_5 species (Merouani et al. 2014c). The number of collapsing bubbles was predicted using Eq. 10 of Table 1. This equation was developed based on a semiempirical method using the results of single-bubble sonochemistry model and some experimental measurements (Merouani et al. 2014a).

Results and discussion

Characterization of the 1700-kHz cavitation field

The bubble dynamics at 1700 kHz of frequency and 15 W of power was performed early for one acoustic cycle (Ferkous et al. 2016). Herein, we will present the results for various acoustic cycles. Figure 1a–e shows the time evolution of the acoustic pressure, the normalized bubble radius, the bubble wall velocity and the bubble pressure and temperature for ten successive implosions. As can be observed, the bubble expands when the acoustic pressure goes negative during the rarefaction cycle up to reaching a maximum ($3.2R_0$) and then violently collapses during the compression cycle of the sound wave. As a result, the speed of the bubble wall hugely increased at the end of each bubble collapse up to values of about 160 m/s, resulting in intense picks of temperature and pressure with maximums of ~ 4000 K and ~ 1000 atm. Dissociation of water vapor, O_2 and N_2 occurred inside the bubble at the final stage of the collapse (around R_{min}), and several chemical oxidants are produced (Merouani et al. 2014c). The amounts of the oxidants reached at the end of the first bubble collapse are given in Fig. 2. As seen from this figure, $^{\cdot}OH$, O and $H^{\cdot}$ are the predominant oxidizing species created at the collapse. In particular, $^{\cdot}OH$ is considered the primary oxidizing species during aqueous sonolysis because of its high potential of oxidation than other oxidants. This reactive species has been identified in sonicated water using EPR-spin trapping (Makino et al. 1982) and has been quantified by several chemical dosimetries (Merouani et al. 2010a).

Figure 3 shows the correspondence between the size of active bubbles (in term of R_0) and the production rate of the oxidants inside the bubbles for 1700 kHz and 15 W. As seen, the range of active bubbles for the production of the oxidants is rather narrow, which is in agreement with an early calculation at various frequencies (Merouani et al. 2013). Only bubbles having ambient radius in the range 0.23–3 µm are active and can produce oxidants, i.e., specifically $^{\cdot}OH$ radical. Additionally, the more active bubbles have an ambient radius of ~ 1.2 µm. The correlation between the yield of $^{\cdot}OH$ and the maximum bubble temperature for all points of Fig. 3 is depicted in Fig. 4. It was noticed that there exists an optimum bubble temperature and pressure of about 4000 K and 1000 atm for the production of hydroxyl radical at 1700 kHz and 15 W.

The predicted number of active bubbles (of 1.2 µm of mean ambient radius) in the cavitating medium is shown in Fig. 5 as function of solution temperature (25–55 °C). As seen, billions of bubbles are created in the medium. From Fig. 5, it was noticed that an increase in bulk liquid temperature leads to a substantial increase in the number

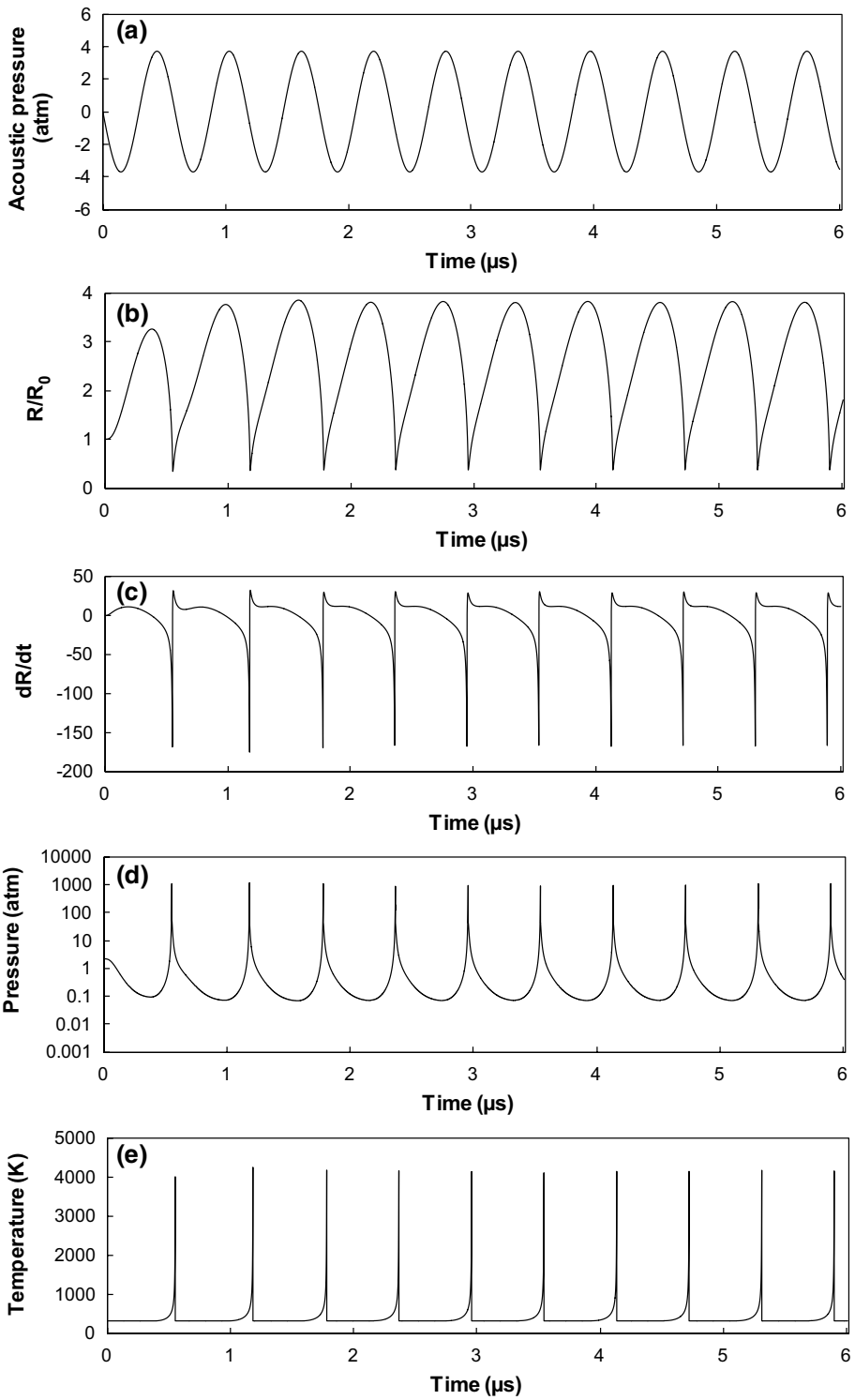

Fig. 1 Predicted acoustic pressure (**a**), normalized bubble radius evolution (**b**), bubble wall velocity (d*R*/d*t*) (**c**) and bubble pressure (**d**) and temperature (**e**) responses during the oscillation of an air bubble in water upon a sound wave at 1700 kHz and 15 W (simulation conditions: ambient bubble radius: 1.2 μm; bulk liquid temperature: 25 °C, static pressure: 1 atm). The vertical axis in **d** is in logarithmic scale

of active bubbles, which suggests that cavitation bubbles are more easily produced as the temperature is raised. This in fact may be due to the decrease in cavitation threshold with the increase in liquid temperature as a result of the rise in vapor pressure or the decrease in either the surface tension or viscosity associated with heating of the liquid (Merouani et al. 2016).

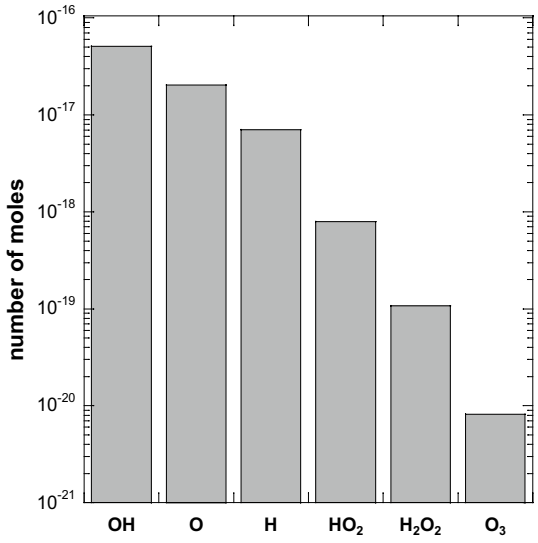

Fig. 2 Amounts of the main oxidants created inside the bubble at the end of the first bubble collapse (conditions—ambient bubble radius: 1.2 µm, liquid temperature: 25 °C, pressure: 1 atm, frequency: 1700 kHz, power: 15 W). Vertical axis is in logarithmic scale

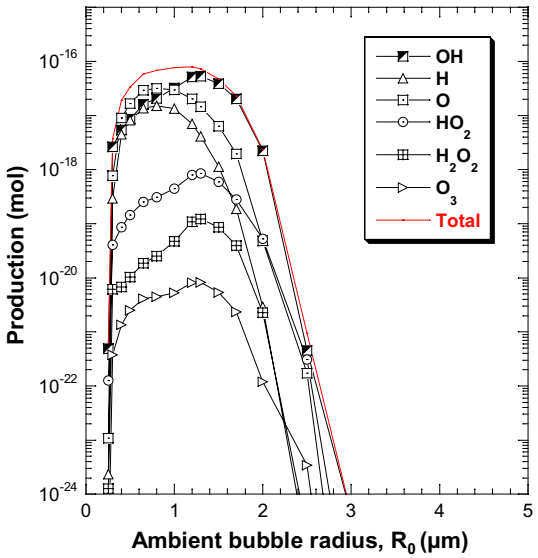

Fig. 3 Size of active bubbles for the production of oxidants (conditions—ambient bubble radius: 0.2–3 µm, liquid temperature: 25 °C, static pressure: 1 atm, frequency: 1700 kHz, power: 15 W)

Application of the 1700-kHz cavitation field to the degradation of TB

The early characterized cavitation field induced at 1700 kHz and 15 W was applied in this section to the degradation of TB, which is a very persistent pollutant toward direct attacks with highly conventional oxidants such as hydrogen peroxide

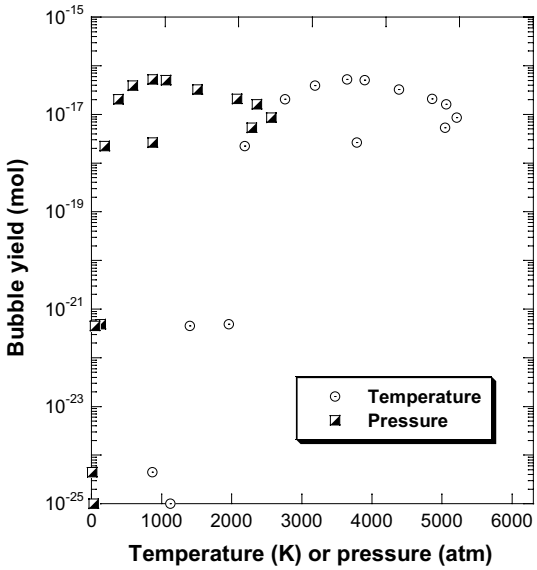

Fig. 4 Bubble yield (hydroxyl radical) as function of the maximum bubble temperature and pressure reached at the collapse for all the interval of active bubbles (conditions—ambient bubble radius: 0.2–3 µm, liquid temperature: 25 °C, static pressure: 1 atm, frequency: 1700 kHz, power: 15 W)

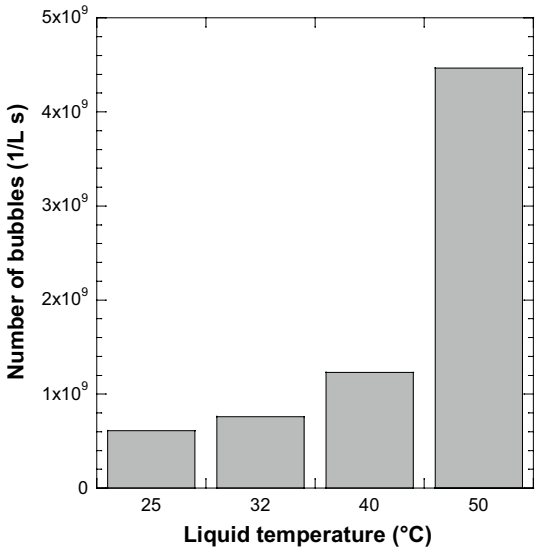

Fig. 5 The number of active bubbles as function of bulk liquid temperature (conditions—ambient bubble radius: 1.2 µm, liquid temperature: 25–50 °C, frequency: 1700 kHz, acoustic power: 15 W)

($E^0_{H_2O_2} = 1.78$ V), persulfate ($E^0_{S_2O_8^{2-}} = 2.01$ V) and periodate ($E^0_{IO_4^-} = 1.6$ V).[1] The potential of cavitation bubbles to generate hydroxyl radicals was verified experimentally with

[1] Experiments were conducted in our laboratory.

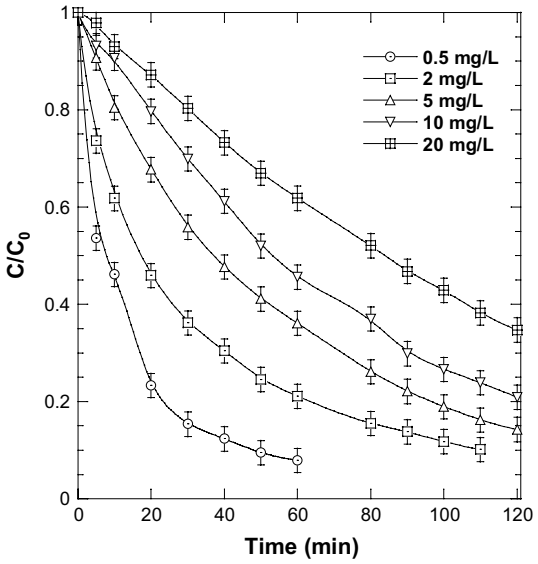

Fig. 6 Degradation kinetics of TB for various initial concentrations (conditions—volume: 100 mL, initial TB concentration: 0.5–20 mg/L, temperature: 25 ± 2 °C, pH ~ 6, frequency: 1700 kHz, power: 15 W)

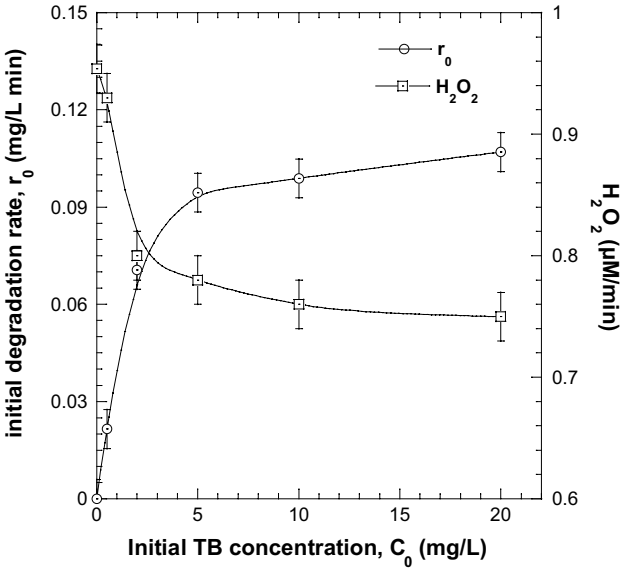

Fig. 7 Initial degradation rate and H_2O_2 formation rate with respect to the initial TB concentration

measuring the production rate of H_2O_2 in the sonicating solution. [H_2O_2 was formed mainly at the bubble–solution interface through the reaction $2\,^{\cdot}OH \rightarrow H_2O_2$ with $k = 5.5 \times 10^{10}\ M^{-1}\ s^{-1}$ (Merouani et al. 2010a)].

Figure 6 shows the impact of the cavitational process on the degradation of TB in aerated solutions of various initial concentrations ($C_0 = 0.5$, 2, 5, 10 and 20 mg/L). The extent of TB degradation was found to be inversely proportional to the initial concentration of the dye, a trend generally observed in the literature (Merouani et al. 2010b; Guzman-Duque et al. 2011; Gao et al. 2013; Ferkous et al. 2015). The variation in the concentration of TB with time showed an exponential decrease resembling a pseudo-first-order kinetics. A quick analysis of Fig. 6 indicates that the degradation extent after 1 h of sonication for the case of $C_0 = 0.5$ mg/L was 1.44 and 2.41 times higher as compared to initial concentrations of 5 and 20 mg/L, respectively (92% at 0.5 mg/L face to 63.8% at 10 mg/L and 38.1% at 20 mg/L). Since TB is highly water soluble [solubility: 38.2 g L^{-1} (Singh et al. 2008)] and nonvolatile substrate [vapor pressure: 1.03×10^{-7} mmHg], it cannot enter the bubble but it must be removed outside by reaction with $^{\cdot}OH$ radical ejected from the bubble. This mechanism was confirmed by adding 2-propanol as an effective $^{\cdot}OH$ scavenger, in which TB removal was hugely reduced (data not shown). Figure 7 depicts the variation in the initial degradation rate (r_0) and H_2O_2 production rate with the initial TB concentration. It can be seen that the initial degradation rate shows two regimes, a linear increase (up to $C_0 = 5$ mg/L) followed with a plateau for all $C_0 > 5$ mg/L. Thus, TB degradation could not be described with a first-order kinetics, as suspected, since there was no linear relation between C_0 and r_0. Therefore, TB degradation is linked to both the TB concentration and hydroxyl radicals. Concurrently, H_2O_2 decreased rapidly from 0.95 μM/min in fresh water to 0.78 μM/min in 5 mg/L TB solution and does not decrease much beyond this concentration (Fig. 7). These results demonstrated the involvement of hydroxyl radical in the degradation of the dye and reflected a saturation of the bubble surface with TB molecules for $C_0 > 5$ mg/L. These findings may be attributed to the difference in the reaction zone with respect to the initial concentration of TB. At low C_0, the bulk solution is the suitable reaction zone (Jiang et al. 2006). It is reported that only 10% of the formed radicals inside the bubbles may reached this zone. In this case, only lower fraction of the $^{\cdot}OH$ radicals may attack TB molecules and the remaining $^{\cdot}OH$ radicals recombine to yield higher formation rate of H_2O_2. However, increasing the pollutant concentration moves progressively the reaction zone to the interfacial region where higher concentration of radicals is believed to be existed (Jiang et al. 2006). In this situation, the fraction of $^{\cdot}OH$ that undergo recombination would decrease (yielding lower accumulation rate of H_2O_2) and be involved in the degradation process, and hence, the degradation rate was ameliorated, as shown in Fig. 7. These remarks are in agreement with those reported in the literature (Torres et al. 2008; Gao et al. 2013; Ferkous et al. 2015; Taamallah et al. 2016).

Figure 8 shows the impact of the cavitational treatment on the removal of TB ($C_0 = 2$ mg/L) in aerated solutions of various initial pH (2–11). As seen, the degradation rate of TB was insignificantly affected upon pH 2–4, but it was

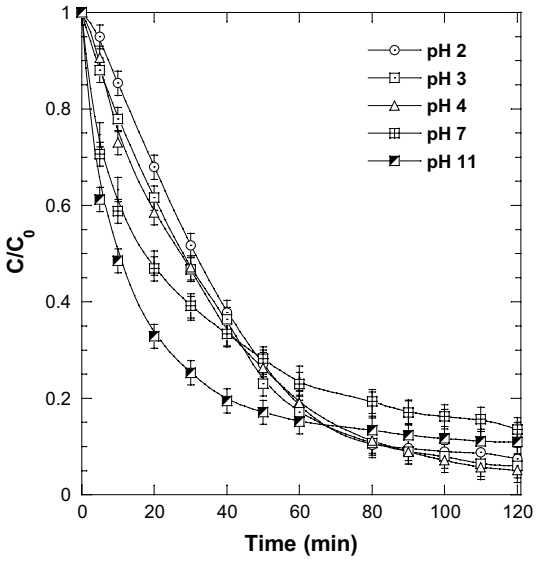

Fig. 8 Degradation kinetics of TB for various initial solution pH (conditions—volume: 100 mL, initial TB concentration: 2 mg/L, temperature: 25 ± 2 °C, pH 2–11, frequency: 1700 kHz, power: 15 W)

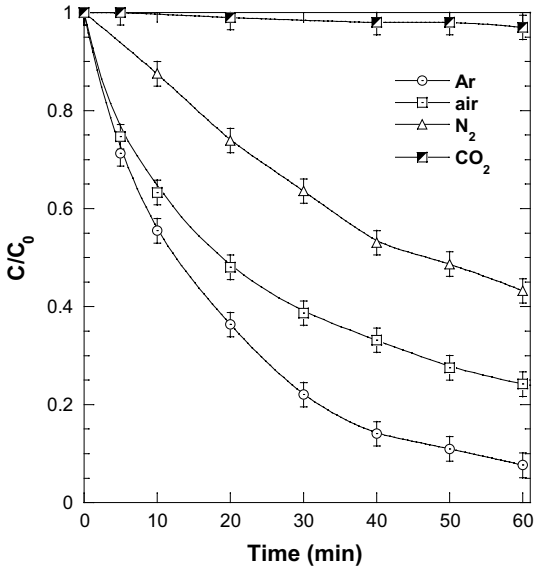

Fig. 9 Degradation kinetics of TB for various saturating gases (conditions—volume: 100 mL, initial TB concentration: 2 mg L^{-1}, temperature: 25 ± 2 °C, pH ~ 6, frequency: 1700 kHz, power: 15 W)

markedly increased in neutral and basic solutions. The initial degradation rate at pH 11 is 1.32-fold higher than that at pH 7. However, after a period of sonolysis (1 h), the degradation of TB at pH 7 and 11 declined and becomes lower than that observed at pH 2–4. This behavior was attributed to the strong competitive effect imposed by the high quantity of degradation by-products resulted from the rapid degradation of TB at neutral and basic conditions. The solution pH may change the acido-basic properties of substances, and this may affect their reactivity toward the cavitation bubble. However, since TB has pKa values of 2.4 and 11.6 (Sabnis 2010), the compound retained the same structural form in the pH range of 2–11. On the other hand, either in the absence or presence of solutes, the formation rate of H_2O_2 was almost independent of pH in the interval 2–11 (Merouani et al. 2010a; Villaroel et al. 2014). Therefore, an opposite trend between the degradation pattern and the production of hydroxyl radical, as quantified by H_2O_2, with respect to pH was obtained. The interpretation of this phenomenon remains obscure, but it may be due to the difference in the number of hydroxyl radicals achieving the bulk solution under lower and higher pH.

Figure 9 shows the effect of the nature of dissolved gases (Ar, air, N_2 and CO_2) on the cavitational treatment of TB ($C_0 = 2$ mg/L). The cavitational treatment is very sensitive to the type of the saturation gas. The degradation rate was more notably under Ar saturation and near completely suppressed under CO_2 atmosphere. Besides, N_2 reduced the degradation rate by 72% and 65%, as compared with Ar and air, respectively. Three main gas properties control the gas effect on the sonochemical process (Rooze et al. 2013): (1) the specific heat ratio ($\gamma = c_p/c_v$), (2) the solubility and (3) the thermal conductivity (λ). A gas with higher solubility (x, mol/mol) can create more nucleation sites, which resulted in higher number of bubbles. On the other hand, a gas with greater γ and lower λ yields higher maximum temperature upon collapse resulting in higher sonochemical activity inside the collapsing bubble. However, measurements of bubble temperatures using methyl radical recombination (MRR) under several saturation gases of the same γ and different λ showed that thermal conductivity had practically no impact on the bubble temperature, and hence, its effect should be neglected (Okitsu et al. 2006). Using our model (Sect. 3), temperatures of 6160 K for Ar, 4030 K for both air and N_2 and 3030 K for CO_2 were predicted at 1700 kHz, 15 W and 25 °C. (These temperatures are in the same order of γ (1.66 for Ar, 1.4 for air and N_2 and 1.29 for CO_2).) Therefore, as Ar is highly water soluble than air and N_2 ($x_{Ar} = 2.748 \times 10^{-5}$, $x_{air} = 1.524 \times 10^{-5}$ and $x_{N_2} = 1.276 \times 10^{-5}$), it could give the best performance toward the degradation of TB via the generation of too high $^{\cdot}OH$ concentration in the reacting medium. On the other hand, since air and N_2 have the same γ and slightly difference in their λ, the reductive effect of nitrogen was mainly attributed to its negative impact on the combustion reaction inside the bubble. Indeed, an early computational analysis demonstrated that the production rate of hydroxyl radical inside the bubble is strongly sensitive to the amount of N_2 trapped in the bubble at the collapse, and the higher the concentration of N_2, the lower the production rate of $^{\cdot}OH$ (Merouani et al. 2014c). It was found that $^{\cdot}OH$ was mainly consumed via the reaction

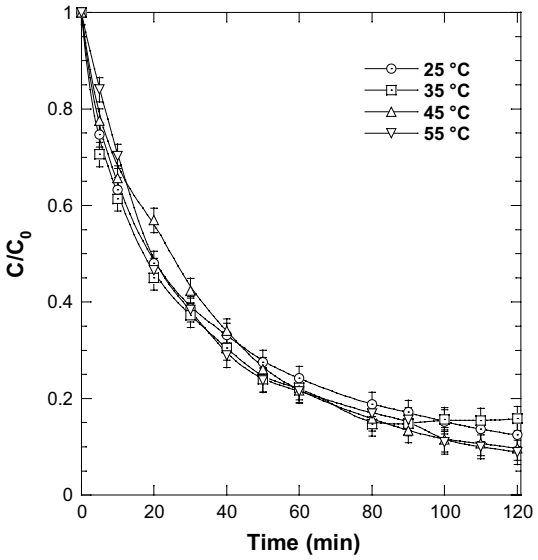

Fig. 10 Degradation kinetics of TB for various solution temperatures (conditions—volume: 100 mL, initial TB concentration: 2 mg/L, temperature: 25–50 °C, pH ~ 6, frequency: 1700 kHz, power: 15 W)

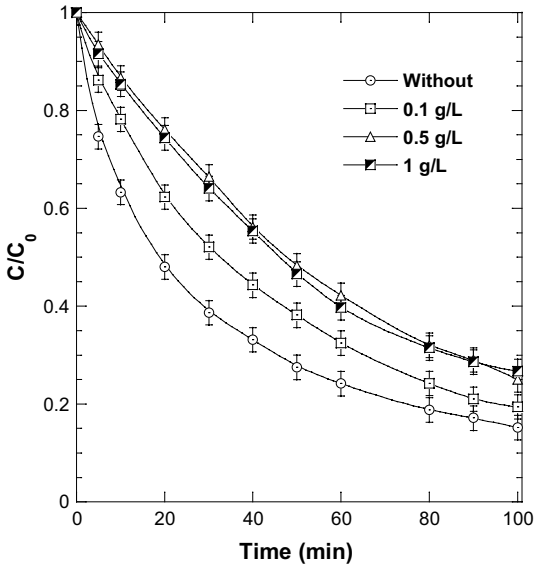

Fig. 11 Effect of formic acid (FA) addition on the degradation kinetics of TB (conditions—volume: 100 mL, initial TB concentration: 20 mg L^{-1}, initial FA concentration: 0.1–1 g L^{-1}, temperature: 25 ± 2 °C, pH ~ 6, frequency: 1700 kHz, power: 15 W)

$NO + {}^{\cdot}OH + M \rightarrow HNO_2 + M$, and since NO was principally formed through the reactions $N_2 + O \rightarrow NO + N$ and $NO_2 + M \rightarrow O + NO + M$, the higher the concentration of N_2 in the bubble, the higher the concentration of NO, and this accelerates the consumption rate of ·OH radical through the reaction $NO + {}^{\cdot}OH + M \rightleftharpoons HNO_2 + M$. For the case of CO_2, the significant lower bubble temperature generated in this case, 3030 K, drastically reduced the production of free radicals at the collapse. Additionally, the too high solubility of CO_2 in water ($x_{CO_2} = 7.1 \times 10^{-4}$; 46-fold much higher than that of air) destabilizes the bubble growth and implosion to a non-inertial event due to the high extent of bubbles coalescence, which yield bigger bubbles in the solution (Brotchie et al. 2010; Rooze et al. 2011). Indeed, images captured of the bubble fields under air and carbon dioxide using a light source demonstrated that the nucleation of bubbles seems to be important for the process (Rooze et al. 2011). Hardly any bubbles are visible in the air-saturated solution, whereas big stable bubbles are visible in the solution under CO_2 saturation (Rooze et al. 2011). The suppressing effect of CO_2 was reported for several chemical and biological processes under ultrasound (Liu and Wu 1934; Henglein 1985; Ogawa et al. 2002; Guzman-Duque et al. 2011).

Figure 10 depicts the effect of liquid temperature (25–55 °C) on the cavitational treatment of TB ($C_0 = 2$ mg/L) in aerated solutions. As can be observed, the liquid temperature had not a significant impact on the removal rate of TB, which is in agreement with the results of Goel et al. (Goel et al. 2004) who investigated the effect of temperature (5–45 °C) on the sono-degradation of styrene and ethylbenzene. Inversely, the production rate of H_2O_2 in pure water was 1, 1.3, 1.5 and 1.8 μM/min for, respectively, 25, 35, 45 and 55 °C, reflecting higher concentration of hydroxyl radical at higher temperatures. These opposite results may be attributed to the hydrophilic character of TB, which make it far from the bubble interface at which the sonochemical activity is mostly located (Jiang et al. 2006). Thus, even increasing liquid temperature acts as enhancer for hydroxyl radical generation, the degradation reaction at the investigated initial concentration (2 mg L^{-1}) will not benefited as TB remains always far from the reactive interfacial region.

Figure 11 shows the effect of formic acid (FA) addition on the cavitational removal of TB ($C_0 = 2$ mg/L) in aerated solutions. It was noticed that FA addition at 0.1 and 0.5 g/L resulted in, respectively, 40% and 60% reduction in the initial removal rate of TB, but no further reduction was observed with 1 g/L of FA. However, FA impacted slowly the removal percentage after a long irradiation time (i.e., ~ 4–10% for 100 min of treatment). These results indicated an effective scavenging of ·OH radical by FA, as experimentally demonstrated by dosing H_2O_2 at variable FA concentrations (Navarro et al. 2011). Although FA is a hydrophilic compound, its reaction with ·OH at high FA concentration levels may occur in both the bubble solution interface and the bulk of the solution (Gogate et al. 2006; Navarro et al. 2011). Since TB reaction zone at $C_0 = 2$ mg/L is presumably the bulk solution, increasing FA concentration increases, in part, the competition for hydroxyl radical reactions in the bulk solution and, in another part, the scavenging of ·OH radicals at the bubble interface and preventing their diffusion to the bulk solution in which TB degradation takes place.

Therefore, lower degradation rate of TB could be generated with increasing FA concentration in the solution. However, due to the rapid occurrence of bubble–collapse event (~0.17 µs at 1700 kHz and 15 W), ·OH diffusion from the acoustic bubble could not be completely suppressed, and this why FA addition at 1 g/L did not yield further reduction as compared to 0.5 g/L. Indeed, an early analysis of acid orange 7 (AO7) degradation in the presence of high concentrations of interfacial agents, i.e., Triton X-100 and Tween 20 surfactants, confirmed the existence of an optimum dose for these additives above which no further reduction in the degradation rate of AO7 was observed (Hamdaoui and Merouani 2017). The optimum reductive dose of surfactants on the production rate of H_2O_2 was also reported (Yim et al. 2002).

Conclusion

Ultrasound via acoustic cavitation event induced in aqueous solution may produce several physical and chemical effects. The degradation of nonvolatile compounds through reaction with the cavitationally generated ·OH radical is one of the most applications of ultrasound in environmental remediation. To better understanding the chemical action of ultrasound in aqueous solution, a characterization of the acoustic cavitation field is highly needed. In this work, the main characteristics of a 1700-kHz cavitation field in water (bubble number and size, bubbles temperatures and pressures and bubbles chemical yields) were determined using a theoretical procedure based on single-bubble sonochemistry model. Subsequently, the degradation of TB, as substrate model of organic pollutants, using the 1700-kHz cavitation field has been achieved at variable experimental conditions and in the presence of formic acid. Ultrasound at 1700 kHz generates cavitational microreactors of high temperatures and pressures, which could be an effective tool to degrade organic pollutants.

References

Ashokkumar M (2011) The characterization of acoustic cavitation bubbles—an overview. Ultrason Sonochem 18:864–872. https://doi.org/10.1016/j.ultsonch.2010.11.016

Bang JH, Suslick KS (2010) Applications of ultrasound to the synthesis of nanostructured materials. Adv Mater 22:1039–1059. https://doi.org/10.1002/adma.200904093

Basturk E, Karatas M (2014) Advanced oxidation of Reactive Blue 181 solution: a comparison between Fenton and Sono-Fenton process. Ultrason Sonochem 21:1881–1885. https://doi.org/10.1016/j.ultsonch.2014.03.026

Bekkouche S, Bouhelassa M, Ben A et al (2017) Synergy between solar photocatalysis and high frequency sonolysis toward the degradation of organic pollutants in aqueous phase—case of phenol. Desalination Water Treat 20146:1–8. https://doi.org/10.5004/dwt.2017.20146

Brotchie A, Statham T, Zhou M et al (2010) Acoustic bubble sizes, coalescence, and sonochemical activity in aqueous electrolyte solutions saturated with different gases. Langmuir 26:12690–12695. https://doi.org/10.1021/la1017104

Chakma S, Moholkar VS (2013) Numerical simulation and investigation of system parameters of sonochemical process. Chin J Eng. https://doi.org/10.1155/2013/362682

Chi Z, Liu R, Sun Y et al (2010) Investigation on the toxic interaction of toluidine blue with calf thymus DNA. J Hazard Mater 175:274–278. https://doi.org/10.1016/j.jhazmat.2009.09.160

Ferkous H, Hamdaoui O, Merouani S (2015) Sonochemical degradation of naphthol blue black in water: effect of operating parameters. Ultrason Sonochem 26:40–47. https://doi.org/10.1016/j.ultsonch.2015.03.013

Ferkous H, Merouani S, Hamdaoui O (2016) Sonolytic degradation of naphthol blue black at 1700 kHz: effects of salts, complex matrices and persulfate. J Water Process Eng 9:67–77. https://doi.org/10.1016/j.str.2014.12.012

Gao YQ, Gao NY, Deng Y et al (2013) Factors affecting sonolytic degradation of sulfamethazine in water. Ultrason Sonochem 20:1401–1407. https://doi.org/10.1016/j.ultsonch.2013.04.007

Goel M, Hongqiang H, Mujumdar AS, Ray MB (2004) Sonochemical decomposition of volatile and non-volatile organic compounds—a comparative study. Water Res 38:4247–4261. https://doi.org/10.1016/j.watres.2004.08.008

Gogate PR, Pandit AB, Wilhelm A et al (2006) Destruction of formic acid using high frequency cup horn reactor. Water Res 40:1697–1705. https://doi.org/10.1016/j.watres.2006.02.011

Guzman-Duque F, Pétrier C, Pulgarin C et al (2011) Effects of sonochemical parameters and inorganic ions during the sonochemical degradation of crystal violet in water. Ultrason Sonochem 18:440–446. https://doi.org/10.1016/j.ultsonch.2010.07.019

Hamdaoui O, Merouani S (2017) Ultrasonic destruction of acid orange 7: effect of humic acid, surfactants and complex matrices. Water Environ Res 89:250–259. https://doi.org/10.2175/106143016X14798353399539

Henglein A (1985) Sonolysis of carbon dioxide, nitrous oxide and methane in aqueous solution. Zeitschrift f{ü}r Naturforsch 40:100–107

Hoffmann MR, Hua I, Höchemer R (1996) Application of ultrasonic irradiation for the degradation of chemical contaminants in water. Ultrason Sonochem 3:S163–S172. https://doi.org/10.1016/S1350-4177(96)00022-3

Jiang Y, Petrier C, Waite TD (2006) Sonolysis of 4-chlorophenol in aqueous solution: effects of substrate concentration, aqueous temperature and ultrasonic frequency. Ultrason Sonochem 13:415–422. https://doi.org/10.1016/j.ultsonch.2005.07.003

Kaur S, Singh V (2007) Visible light induced sonophotocatalytic degradation of Reactive Red dye 198 using dye sensitized TiO2. Ultrason Sonochem 14:531–537. https://doi.org/10.1016/j.ultsonch.2006.09.015

Liu S-C, Wu H (1934) Mechanism of oxidation promoted by ultrasonic radiation. J Am Chem Soc 56:1005–1007. https://doi.org/10.1021/ja01320a001

Makino K, Mossoba MM, Riesz P (1982) Chemical effects of ultrasound on aqueous solutions. Evidence for ·OH an ·H by

spin trapping. J Am Chem Soc 104:3537–3539. https://doi.org/10.1021/ja00376a064
Malani RS, Khanna S, Chakma S, Moholkar VS (2014) Mechanistic insight into sono-enzymatic degradation of organic pollutants with kinetic and thermodynamic analysis. Ultrason Sonochem 21:1400–1406. https://doi.org/10.1016/j.ultsonch.2014.01.028
Mason TJ, Lorimer JP, Bates DM (1992) Quantifying sonochemistry: casting some light on a "black art". Ultrasonics 30:40–42. https://doi.org/10.1016/0041-624X(92)90030-P
Merouani S, Hamdaoui O (2017) Computational and experimental sonochemistry. Process Eng J 1:10–18
Merouani S, Hamdaoui O, Saoudi F, Chiha M (2010a) Influence of experimental parameters on sonochemistry dosimetries: KI oxidation, Fricke reaction and H_2O_2 production. J Hazard Mater 178:1007–1014. https://doi.org/10.1016/j.jhazmat.2010.02.039
Merouani S, Hamdaoui O, Saoudi F, Chiha M (2010b) Sonochemical degradation of Rhodamine B in aqueous phase: effects of additives. Chem Eng J 158:550–557. https://doi.org/10.1016/j.cej.2010.01.048
Merouani S, Hamdaoui O, Rezgui Y, Guemini M (2013) Effects of ultrasound frequency and acoustic amplitude on the size of sonochemically active bubbles—theoretical study. Ultrason Sonochem 20:815–819. https://doi.org/10.1016/j.ultsonch.2012.10.015
Merouani S, Ferkous H, Hamdaoui O et al (2014a) A method for predicting the number of active bubbles in sonochemical reactors. Ultrason Sonochem 22:51–58. https://doi.org/10.1016/j.ultsonch.2014.07.015
Merouani S, Hamdaoui O, Rezgui Y, Guemini M (2014b) Theoretical procedure for the characterization of acoustic cavitation bubbles. Acta Acust United Acust 100:823–833. https://doi.org/10.3813/AAA.918762
Merouani S, Hamdaoui O, Rezgui Y, Guemini M (2014c) Sensitivity of free radicals production in acoustically driven bubble to the ultrasonic frequency and nature of dissolved gases. Ultrason Sonochem 22:41–50. https://doi.org/10.1016/j.ultsonch.2014.07.011
Merouani S, Hamdaoui O, Rezgui Y, Guemini M (2015) Mechanism of the sonochemical production of hydrogen. Int J Hydrogen Energy 40:4056–4064. https://doi.org/10.1016/j.ijhydene.2015.01.150
Merouani S, Hamdaoui O, Boutamine Z et al (2016) Experimental and numerical investigation of the effect of liquid temperature on the sonolytic degradation of some organic dyes in water. Ultrason Sonochem 28:382–392. https://doi.org/10.1016/j.ultsonch.2015.08.015
Moholkar VS, Warmoeskerken MMCG (2003) Integrated approach to optimization of an ultrasonic processor. AIChE J 49:2918–2932. https://doi.org/10.1002/aic.690491121
Moholkar VS, Rekveld S, Warmoeskerken MMCGCG (2000a) Modeling of the acoustic pressure fields and the distribution of the cavitation phenomena in a dual frequency sonic processor. Ultrasonics 38:666–670. https://doi.org/10.1016/S0041-624X(99)00204-8
Moholkar VS, Sable SP, Pandit AB (2000b) Mapping the cavitation intensity in an ultrasonic bath using the acoustic emission. AIChE J 46:684–694. https://doi.org/10.1002/aic.690460404
Navarro NM, Chave T, Pochon P et al (2011) Effect of ultrasonic frequency on the mechanism of formic acid sonolysis. J Phys Chem B 115:2024–2029. https://doi.org/10.1021/jp109444h
Nazimudheen G, Roy K, Sivasankar T, Moholkar VS (2018) Mechanistic investigations in ultrasonic pretreatment and anaerobic digestion of landfill leachates. J Environ Chem Eng 6:1690–1701. https://doi.org/10.1016/j.jece.2018.02.001
Neelakandeswari N, Sangami G, Dharmaraj N et al (2011) Spectroscopic investigations on the photodegradation of toluidine blue dye using cadmium sulphide nanoparticles prepared by a novel method. Spectrochim Acta Part A Mol Biomol Spectrosc 78:1592–1598. https://doi.org/10.1016/j.saa.2011.02.008
Neppiras EAA (1980) Acoustic Cavitation. Phys Rep 61:1–11. https://doi.org/10.1016/0370-1573(80)90115-5
Ogawa R, Kondo T, Honda H et al (2002) Effects of dissolved gases and an echo contrast agent on ultrasound mediated in vitro gene transfection. Ultrason Sonochem 9:197–203. https://doi.org/10.1016/S1350-4177(02)00075-5
Okitsu K, Suzuki T, Takenaka N et al (2006) Acoustic multibubble cavitation in water: a new aspect of the effect of a rare gas atmosphere on bubble temperature and its relevance to sonochemistry. J Phys Chem B 110:20081–20084. https://doi.org/10.1021/jp064598u
Park B, Qiu P, Thokchom B et al (2018) Mechanistic investigations in sonochemical degradation of trihalomethanes in presence of non–porous and mesoporous silica nanospheres. J Water Process Eng 24:26–34. https://doi.org/10.1016/j.jwpe.2018.05.005
Peller J, Wiest O, Kamat PV (2003) Synergy of combining sonolysis and photocatalysis in the degradation and mineralization of chlorinated aromatic compounds. Environ Sci Technol 37:1926–1932. https://doi.org/10.1021/es0261630
Pétrier C, Francony A (1997) Ultrasonic waste-water treatment: incidence of ultrasonic frequency on the rate of phenol and carbon tetrachloride degradation. Ultrason Sonochem 4:295–300. https://doi.org/10.1016/S1350-4177(97)00036-9
Petrier C, Jiang Y, Lamy MF (1998) Ultrasound and environment: sonochemical destruction of chloroaromatic derivatives. Environ Sci Technol 32:1316–1318. https://doi.org/10.1021/es970662x
Pollet BG (2010) The use of ultrasound for the fabrication of fuel cell materials. Int J Hydrogen Energy 35:11986–12004. https://doi.org/10.1016/j.ijhydene.2010.08.021
Rooze J, Rebrov EV, Schouten JC, Keurentjes JTF (2011) Effect of resonance frequency, power input, and saturation gas type on the oxidation efficiency of an ultrasound horn. Ultrason Sonochem 18:209–215. https://doi.org/10.1016/j.ultsonch.2010.05.007
Rooze J, Rebrov EV, Schouten JC, Keurentjes JTF (2013) Dissolved gas and ultrasonic cavitation—a review. Ultrason Sonochem 20:1–11. https://doi.org/10.1016/j.ultsonch.2012.04.013
Sabnis RW (2010) Handbook of biological dyes and stains: synthesis and industrial applications. Wiley, Hoboken
Sáez V, Esclapez MD, Tudela I et al (2010) 20 kHz sonoelectrochemical degradation of perchloroethylene in sodium sulfate aqueous media: Influence of the operational variables in batch mode. J Hazard Mater 183:648–654. https://doi.org/10.1016/j.jhazmat.2010.07.074
Serpone N, Colarusso P (1994) Sonochemistry I. Effects of ultrasounds on heterogeneous chemical reactions—a useful tool to generate radicals and to examine reaction mechanisms. Res Chem Intermed 20:635–679. https://doi.org/10.1163/156856794X00261
Singh HK, Saquib M, Haque MM, Muneer M (2008) Heterogeneous photocatalysed decolorization of two selected dye derivatives neutral red and toluidine blue in aqueous suspensions. Chem Eng J 136:77–81. https://doi.org/10.1016/j.cej.2007.05.009
Sivasankar T, Paunikar AW, Moholka VS (2007) Mechanistic approach to enhancement of the yield of a sonochemical reaction. AIChE J 53:1132–1143. https://doi.org/10.1002/aic
Sridharan G, Shankar A (2012) Toluidine blue: a review of its chemistry and clinical utility. J Oral Maxillofac Pathol 16:251–255. https://doi.org/10.4103/0973-029X.99081
Suslick KS, Hammerton DA, Cline JRE, Cline RE (1986) The sonochemical hot spot. J Am Chem Soc 108:5641–5642. https://doi.org/10.1021/ja00278a055
Taamallah A, Merouani S, Hamdaoui O (2016) Sonochemical degradation of basic fuchsin in water. Desalination Water Treat. https://doi.org/10.1080/19443994.2016.1168320
Teo BM, Ashokkumar M, Grieser F (2008) Microemulsion polymerizations via high-frequency ultrasound irradiation. J Phys Chem B 112:5265–5267. https://doi.org/10.1021/jp801536u

Teo BM, Grieser F, Ashokkumar M (2009) High intensity ultrasound initiated polymerization of butyl methacrylate in mini- and microemulsions. Macromolecules 42:4479–4483. https://doi.org/10.1021/ma900521z

Torres RA, Pétrier C, Combet E et al (2008) Ultrasonic cavitation applied to the treatment of bisphenol A. Effect of sonochemical parameters and analysis of BPA by-products. Ultrason Sonochem 15:605–611. https://doi.org/10.1016/j.ultsonch.2007.07.003

Verma A, Kaur Hura A, Dixit D (2015) Sequential photo-Fenton and sono-photo-Fenton degradation studies of Reactive Black 5 (RB5). Desalination Water Treat 56:677–683. https://doi.org/10.1080/19443994.2014.940390

Vichare NP, Senthilkumar P, Moholkar VS et al (2000) Energy analysis in acoustic cavitation. Ind Eng Chem Res 39:1480–1486. https://doi.org/10.1021/ie9906159

Villaroel E, Silva-Agredo J, Petrier C et al (2014) Ultrasonic degradation of acetaminophen in water: effect of sonochemical parameters and water matrix. Ultrason Sonochem 21:1763–1769. https://doi.org/10.1016/j.ultsonch.2014.04.002

Xue B (2016) Ultrasonic synthesis of nanomaterials for photocatalytic removal of wastewater. In: Handbook of ultrasonics and sonochemistry. Springer, Singapore

Yasui K, Tuziuti T, Sivakumar M, Iida Y (2005) Theoretical study of single-bubble sonochemistry. J Chem Phys 122:224706. https://doi.org/10.1063/1.1925607

Yim B, Okuno H, Nagata Y et al (2002) Sonolysis of surfactants in aqueous solutions: an accumulation of solute in the interfacial region of the cavitation bubbles. Ultrason Sonochem 9:209–213. https://doi.org/10.1016/S1350-4177(01)00123-7